



**HAL**  
open science

## Replacing silver by aluminum in solar mirrors by improving solar reflectance with dielectric top layers

Antoine Grosjean, Audrey Soum-Glaude, Laurent Thomas

### ► To cite this version:

Antoine Grosjean, Audrey Soum-Glaude, Laurent Thomas. Replacing silver by aluminum in solar mirrors by improving solar reflectance with dielectric top layers. *Sustainable Materials and Technologies*, 2021, 29, pp.e00307. 10.1016/j.susmat.2021.e00307 . hal-03368709

**HAL Id: hal-03368709**

**<https://univ-perp.hal.science/hal-03368709>**

Submitted on 2 Aug 2023

**HAL** is a multi-disciplinary open access archive for the deposit and dissemination of scientific research documents, whether they are published or not. The documents may come from teaching and research institutions in France or abroad, or from public or private research centers.

L'archive ouverte pluridisciplinaire **HAL**, est destinée au dépôt et à la diffusion de documents scientifiques de niveau recherche, publiés ou non, émanant des établissements d'enseignement et de recherche français ou étrangers, des laboratoires publics ou privés.



Distributed under a Creative Commons Attribution - NonCommercial 4.0 International License

# Replacing silver by aluminum in solar mirrors by improving solar reflectance with dielectric top layers

Antoine Grosjean<sup>1,2</sup>, Audrey Soum-Glaude<sup>3,\*</sup>, Laurent Thomas<sup>1,2</sup>

<sup>1</sup> PROMES-CNRS, UPR 8521, Rambla de la thermodynamique, Tecnosud, 66100 Perpignan, France.

<sup>2</sup> Université de Perpignan, 52 avenue Paul Alduy, 66820 Perpignan, France.

<sup>3</sup> PROMES-CNRS, UPR 8521, 7 rue du Four Solaire, 66120 Font-Romeu-Odeillo-Via, France.

\*corresponding author: [audrey.soum-glaude@promes.cnrs.fr](mailto:audrey.soum-glaude@promes.cnrs.fr)

## ACKNOWLEDGMENTS

This work was supported by the French "Investments for the future" program managed by the National Agency for Research under contract ANR-10-LABX-22-01-SOLSTICE. The authors would like to thank Florian Sutter from DLR for providing incidence angle distribution charts.

# Replacing silver by aluminum in solar mirrors by improving solar reflectance with dielectric top layers

**Abstract:** Silver is a strategic material for renewable energy. Among other applications related to PV, it is used as reflective layer in solar mirrors for concentrated solar power (CSP), thanks to its high reflectance in the whole solar range. CSP plants require large mirror areas, typically in the 0.1 to 1 km<sup>2</sup>. However the estimated reserves of silver do not exceed 20 years. To sustain the deployment of CSP as a valuable input in the future energy mix, silver must be replaced with a less critical material, ideally low cost. In this theoretical study we propose to replace silver by aluminum, adding a dielectric multilayer coating on top, to reach similar optical performance. This design is inspired by Bragg mirrors but differs in that the stack parameters (layer thicknesses) are individually optimized, so as to maximize solar reflectance. A thin aluminum layer with MgF<sub>2</sub>/TiO<sub>2</sub> aperiodic stack on top can theoretically reach solar reflectance of 96.1%, higher than silver (95.5%). Other materials are also found suitable: SiO<sub>2</sub>, ZnO, ZrO<sub>2</sub>. A reasonable number of layers (< 20) not only enhances the optical performance of metallic reflectors, but also allows tuning said performance, which is not possible with classical mirrors relying on a single metal reflective layer. For instance, one can optimize the stack to reach a better performance than silver at typical mean incidence angles of solar light in CSP plants, for different locations. A solar mirror without rare or precious materials and more effective than traditional silver mirrors is thus obtained.

**Keywords:** *Concentrated solar energy, solar mirrors, coating optimization, dielectric layers*

## 1. INTRODUCTION

Solar energy is a very promising way to produce clean, cheap and sustainable electric resource for humankind. The goal is to convert part of the radiative energy coming from the sun, directly into electric energy with a photovoltaic (PV) module, or into heat with a solar concentrator (which can in turn be converted into electricity via a turbine). PV modules have lower prices than Concentrated Solar Power (CSP) technologies, while the main advantage of CSP is that heat can easily be stored on a large scale for a low cost, giving access to electricity-on-demand services. These two solar technologies can thus have a positive impact on territory management, for both developing and industrialized countries. For the former, solar technologies can help increase access to energy and electricity, and what is more, low cost and renewable ones. For the latter, the demand for low carbon emission energy is growing, as most of these countries are committed to reducing their greenhouse gas (GHG) emissions. These advantages led to promote the installation of PV and CSP solar technologies, and the demand continues to grow. Researchers therefore have to focus their attention into developing more efficient and lower cost electrical energy [1]. Yet, PV and CSP are both based on the use of solar collectors,

made of materials such as glass, silicon, and metals. Some of these materials, like silver, are expensive and could rarefy in the near future. Indeed, silver already has an important role in all solar technologies and will have an even more important role in the decades to go, as these technologies expand [2].

Indeed, in photovoltaic technologies, mainly in crystalline silicon solar cells, silver is used in the PV module to form electrical contacts between the cells, due to its high electrical conductivity [3]. According to the worldwide supply and demand for silver, the demand for silver ore for PV was 2.400 tons in 2018 [3]. Between 2017 and 2019, the total year-on-year growth of silver demand was around 19% [4].

In all CSP technologies (solar tower, parabolic trough, linear Fresnel reflectors), silver is also an essential component, for solar reflectors. Indeed, silver is a very powerful reflector which allows reflecting up to 95% of solar energy. It thus allows concentrating efficiently the solar radiation, on a linear or punctual thermal absorber. Commercial silver mirrors for CSP typically have a solar reflectance around 92.5 to 95.5% [5]. The other possible metal for solar mirrors, although much less used, is aluminum, with a lower solar reflectance, close to 86-91% [6], [7]. Other types of mirrors exist, like polymer mirrors, but these still use silver as reflective layers [8], [9]. Currently, solar mirrors use these two metals as thin metallic layers, protected from corrosion by a thin or thick glass [10], by sol-gel coatings of SiO<sub>2</sub> and/or TiO<sub>2</sub> [11], or by a transparent polymer layer on one side and different paints on the other side [12]. The required quantity of silver per mirror is around 1 g/m<sup>2</sup>, and this is without considering material loss inherent to Physical Vapor Deposition (PVD) techniques. Indeed, silver thin layers are deposited in vacuum chambers on glass substrates, but during this process silver is also lost on the chamber walls. This quantity of silver per m<sup>2</sup> must be linked to the solar field area, which can reach hundreds of thousands of m<sup>2</sup> per solar plant. As an example, a typical CSP plant like Andasol-1 (parabolic trough in Spain) has a surface of installed mirrors of 510,120 m<sup>2</sup> to generate 158 GWh/y (with a 7.5 hour thermal storage).

Moreover, solar energy is not the only industrial sector that requires silver utilization. Other applications have been reported, such as medical healthcare, digital technologies, jewelry and safe investments for banks and countries [13–17].

According to the United States Geological Survey (USGS), around 27,000 tons of silver (65<sup>th</sup> most abundant metal) have been extracted from mines in 2018 [18]. As the evaluation of the total world reserve is 560,000 tons, it is around 21 years of total reserve before extinction: so silver can be considered as a critical resource for human development. The maximum production peak of silver is very close, studies give an estimation in the range of 2025-2030 [19,20]. These scenarios do not even consider an exponential growth of usage, or market prices mechanisms such as the choice of silver as financial investments (safe haven value). As it rarefies, silver prices will rise and it is important to consider increasing its recycling, and ideally its substitution with other metals, in particular to ensure low prices and viability of solar energy in the decades to come.

In summary, silver has an important role to play in the green revolution and the total reserve of silver cannot supply the predicted development trends [19,21]. If we look at the current trend for silver production against the growing market of solar technologies, thanks to their lower prices and the need for low cost energies in developing countries, we must consider the critical

question of silver supply. In a study written in 2014, the authors evaluate the silver supply risk for the solar sector, for photovoltaic and solar thermal, as a crucial question [22].

The PV sector takes this problem seriously, with the goal to reduce the quantity of silver in electrical contacts from an average of 130 mg per cell in 2016 to 65 mg per cell by 2028-2030 [19]. Efforts have been made to substitute silver with other materials, which has been an additional point in the cost reduction observed in the past decade [23]. Even if these results are promising, experts in the field agree that the total substitution of silver is still an unresolved matter for the forthcoming years [24], particularly since one must consider the existing and foreseen impressive growth of the PV market and the quantity of silver it will mobilize before a replacement can be found.

In the CSP sector, industrial aluminum-based mirrors are already on the market, like the Miro-Sun<sup>®</sup> from Alanod [25], but these mirrors have a lower solar reflectance compared to silver ones. So even if aluminum mirrors exist, silver mirrors remain the most important part of the CSP mirror market, because of their higher solar reflectance. R&D efforts must thus be made in the field of CSP mirrors to replace or render more profitable the use of silver.

In this context, the main goal of this paper is to prospect, by means of optical simulation, for alternative reflective coatings, adapted to all CSP technologies: either able to reach the same solar reflectance than with silver mirrors but without having recourse to silver; or to reach higher solar performance using silver, to produce more energy with the same amount of silver. Reflective properties are directly linked to refractive index properties, and silver is the best solar reflector in regard of its optical constants. Therefore, substituting the thin layer of silver in solar mirrors by that of another metal would necessarily have a negative impact on solar reflectance. Thus solar performance for mirrors has not progressed significantly for decades. Instead our study is based on adding optimized thin dielectric layers on top of the Al and Ag reflectors, to increase their solar reflectance. Additional layers can indeed provide advanced surface functionalization to modify the optical behavior of a material, much like spectrally selective or antireflective coatings [26–28]. For this purpose, we have simulated, from spectral refractive indices and using the well-known transfer matrix method, the spectral and solar reflectances of two metal reflectors (aluminum and silver) covered with an arrangement of thin dielectric layers on top. The latter were optimized in terms of their thicknesses so as to maximize solar performance, using an in-house optimization algorithm. Various dielectric materials and conditions of use, in particular light incidence angles, were considered. The results were systematically compared to the cases of simple silver and aluminum reflectors to highlight the increased performance provided by the suggested solutions.

## **2. THEORETICAL BACKGROUND AND SIMULATION METHOD**

### **2.1. Spectral properties calculation by Transfer Matrix Method**

This study focuses on stacks of several nanometric thin layers deposited on a substrate. To evaluate the solar performance of these stacks, the calculation of their spectral optical properties, reflectance, transmittance and absorptance is necessary. To calculate the latter, a conventional method known as the Transfer Matrix Method (TMM) was used. This method based on Fresnel equations has been detailed in the literature [29–31]. The high number of optical interfaces between the substrate, the layers and the ambient medium (typically air), creates constructive and

destructive interference that can be estimated using TMM. It requires the knowledge of spectral complex refractive indices of all constitutive materials, which describe the material optical behavior. A characteristic matrix representing the reflection and transmission of each interface is calculated. It takes into account the wavelength  $\lambda$  and impact angle  $\theta$  of the incident light, as well as the complex refractive index and thickness of the layers on each side of the interface. These characteristic matrices are multiplied in sequence to obtain the transfer matrix and calculate the total power reflected  $R(\lambda)$  and transmitted  $T(\lambda)$  by the stack, at each wavelength  $\lambda$  of interest, e.g., over the solar spectrum in our case. The absorbed power  $A(\lambda)$  is deduced from the energy conservation law ( $A(\lambda) = 1 - R(\lambda) - T(\lambda)$ ). In the case of mirrors, the reflector materials are thick enough to be opaque, so there is no transmittance.

## 2.2. Solar reflectance

The stack reflectance spectrum  $R(\lambda)$  can then be weighted by the solar spectrum  $J(\lambda)$  and integrated over wavelength, to calculate the total solar power (in  $\text{W/m}^2$ ) reflected by the stack. This value is divided by the total power received from the Sun, to obtain the solar-weighted reflectance  $R_S$  (expression (1)). The chosen solar spectrum is the ASTM G173-03 AM 1.5 Direct and Circumsolar (DC) defined between 280 and 4000 nm [32,33]. Only the DC solar spectrum is considered and not the Global Tilt (GT) solar spectrum, as diffuse sunlight coming from the ground or clouds cannot be concentrated, and is thus not taken into account in CSP applications [26]. The spectral ranges from 280 to 320 nm and from 2500 to 4000 nm can be ignored, due to the low irradiance in these ranges: they represent less than 1% of the total solar incident power. This reduced spectral range is in fact recommended by SolarPACES organization in solar reflectance guidelines [34].

$$R_S = \frac{\int_{320 \text{ nm}}^{2500 \text{ nm}} R(\lambda) \cdot J(\lambda) \cdot d\lambda}{\int_{320 \text{ nm}}^{2500 \text{ nm}} J(\lambda) \cdot d\lambda} \quad (1)$$

SolarPACES guidelines also recommend the use of a wavelength step  $d\lambda = 5$  nm, since metallic mirrors (Al and Ag) have a stable spectral reflectance. However the spectral reflectance of Ag or Al mirrors with additional dielectric top layers is much more wavelength-dependent, with the existence of several absorption peaks. Thus as a comparison smaller wavelength steps for solar reflectance calculation, i.e., 2 nm, 1 nm and 0.5 nm, were also tested. The difference between the minimum and maximum values of solar reflectance calculated with these steps is lower than 0.01%, so a larger step has no impact on the accuracy of solar reflectance. Also, Heimsath et al. [35] found no studies in the literature that suggest that the amount of scattering and specular reflection of mirrors with additional dielectric layers should differ from that of other mirrors.

## 2.3. Simulation and optimization method

Simulations have been carried out with an in-house numerical code written on Scilab software, version 5.5 [36]. First, the stack is described by choosing the constitutive materials and a min-max thickness range for each layer of the stack (e.g. from 0 to 200 nm, typical of optical coatings). The aim is to maximize the stack solar reflectance by optimizing the thickness of each

layer (included in the initial min-max range). For each thickness tested, the TMM is used to evaluate spectral reflectance in the solar range (from 320 nm to 2500 nm), with a step of 5 nm. This step value provides good accuracy in the solar spectrum domain with a reasonable calculation time for optimization.

The optimization method is based on an in-house algorithm, which proceeds by iteration until convergence of several variables giving the solution. Our optimization method is very similar to a genetic algorithm [37,38]. The algorithm initially generates a large number ( $> 100$ ) of stacks with random layer thicknesses (in the selected min-max range), evaluates their solar reflectance, selects the stacks with highest solar reflectance, creates a new generation, evaluates their solar reflectance, selects the best stacks, etc.; as the selected stacks become more and more efficient after each iteration, a convergence is finally obtained, i.e., the solution.

The computer used for the simulation is equipped with an Intel Xeon E5-2670 processor with 16 threads (virtual CPU cores) and 32 GB of flash memory, to reduce calculation time (few seconds for 2 layers, 4-5 min for 20 layers in the simulated stack). A more standard computer (e.g. 4 cores, 16 GB) would give longer calculation times (e.g. 30 to 60 minutes for 20 layers).

#### 2.4. Complex refractive indices of constitutive materials

The spectral complex refractive indices  $N(\lambda) = n(\lambda) + ik(\lambda)$  of all materials of the stack, including the substrate, are needed for the calculation of spectral reflectance. The complex refractive index  $N(\lambda)$  is made of a real part, the refractive index  $n(\lambda)$ , and an imaginary part, the extinction coefficient ( $k(\lambda)$ ), and describes the material optical behavior. Refractive indices were selected from the following studies available in the literature: for Ag and Al, from Rakic et al. [39]; for  $MgF_2$ , from Dodge et al. [40]; for  $SiO_2$ , from Lemarchant et al. [41]; for ZnO, from Bond et al. [42]; for  $ZrO_2$ , from Wood and Nassau [43]; for  $TiO_2$ , from Siefke [44]; for GaAs, from Rakic et al. [45]. These materials were selected for their suitable refractive index, their good transparency ( $k = 0$ ) and because they are already used in other kinds of optical stacks, such as antireflective coatings for glasses, lasers, etc. [46].

These particular studies were selected according to our scientific objectives, to be as close to real CSP applications as possible: refractive indices were measured on actual samples instead of simulated; the materials were in the form of thin films and not bulk materials; their fabrication technique was similar to that used in CSP industries (sol-gel, physical or chemical vapor deposition). Also, refractive indices were available in the reduced solar spectral range of interest (320 nm – 2500 nm), with enough values to match or approach the chosen 5 nm precision step, i.e., several hundred values in this domain. Linear interpolation with a 5 nm step was applied to fit the data when necessary.

Figure 1 illustrates the spectral refractive indices  $n(\lambda)$  of the selected materials in the solar domain.  $MgF_2$  and  $SiO_2$  have a very stable refractive index in this range, which slowly decreases as wavelength increases.  $TiO_2$  and GaAs have the highest refractive index (respectively up to 3.5 and up to 5) with variations in the UV range. ZnO and  $ZrO_2$  have intermediate refractive index, included between  $SiO_2$  and  $TiO_2$ . Their refractive index is very constant with a slow decrease. In their case, data in the UV range (320 - 400 nm) was not available in the chosen studies, therefore the missing data was linearly extrapolated and validated by comparison with measurements from other studies, where only the UV and visible range was measured [47,48]. Concerning their

absorption coefficient  $k$ , MgF<sub>2</sub>, SiO<sub>2</sub>, ZnO, ZrO<sub>2</sub> and TiO<sub>2</sub> are mainly transparent in the solar domain ( $k < 10^{-4}$ ). Only GaAs absorbs light, especially at lower wavelengths ( $k > 1$  from 280 to 450 nm).

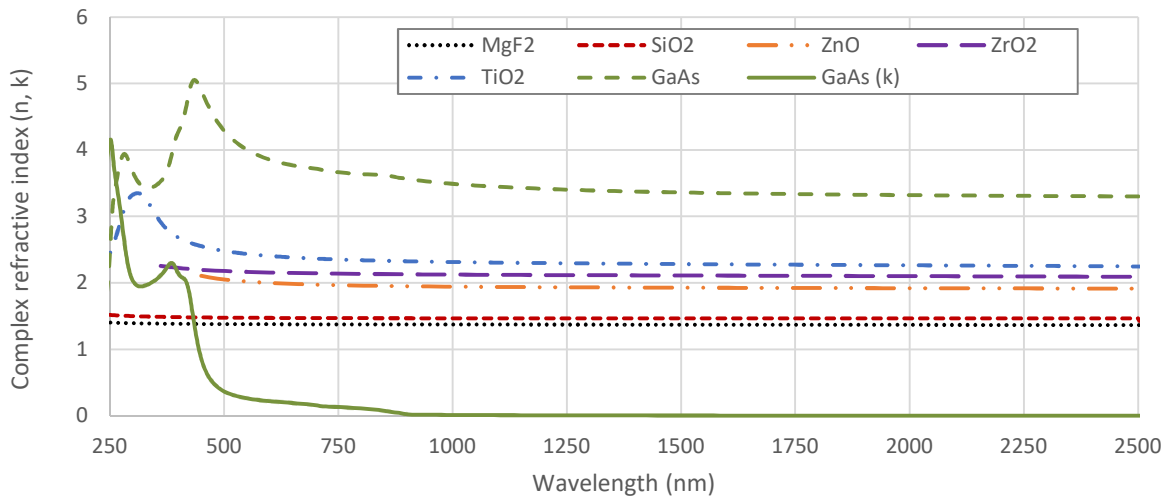


Figure 1 : Refractive indices of MgF<sub>2</sub>, SiO<sub>2</sub>, ZnO, ZrO<sub>2</sub>, TiO<sub>2</sub> and GaAs in the solar domain

### 3. RESULTS AND DISCUSSION

#### 3.1. Pure metal mirrors

As a starting point, the spectral and solar reflectance of silver and aluminum mirrors were evaluated from the refractive indices proposed by Rakic [39]. Commercial Ag and Al CSP mirrors are often made of glass substrates with thin layers of metallic reflectors. These metals being highly opaque, a layer of only 100 - 150 nm has the same optical behavior as bulk metal. Thus to simplify our calculation, these metals were here considered as stand-alone materials, i.e., substrates. All following calculations considering Ag and Al as substrates are equivalent to that considering Ag and Al as thin opaque reflector layers.

Spectral reflectance for Ag and Al are represented in Figure 2 by the dotted red line and solid green line, respectively. Silver has a higher spectral reflectance than aluminum, except in the UV region (280 - 400 nm) where Ag does not reflect. The corresponding solar reflectance, calculated according to ASTM G173-03 DC solar spectrum, is 95.5% for Ag and 92.2% for Al. These values are close to that of commercial products (see section 1), although the latter are smaller by a few % than the theoretical ideal values for pure metals without any defects. Also, commercial mirrors use thin or thick layers of glass above the metallic layer for its protection, and that glass is responsible for some solar absorptance [26]. It is as well due to the quality of the metal deposited, as authors with a specific deposition method can obtain silver layers with a solar reflectance up to 98.5% [49].

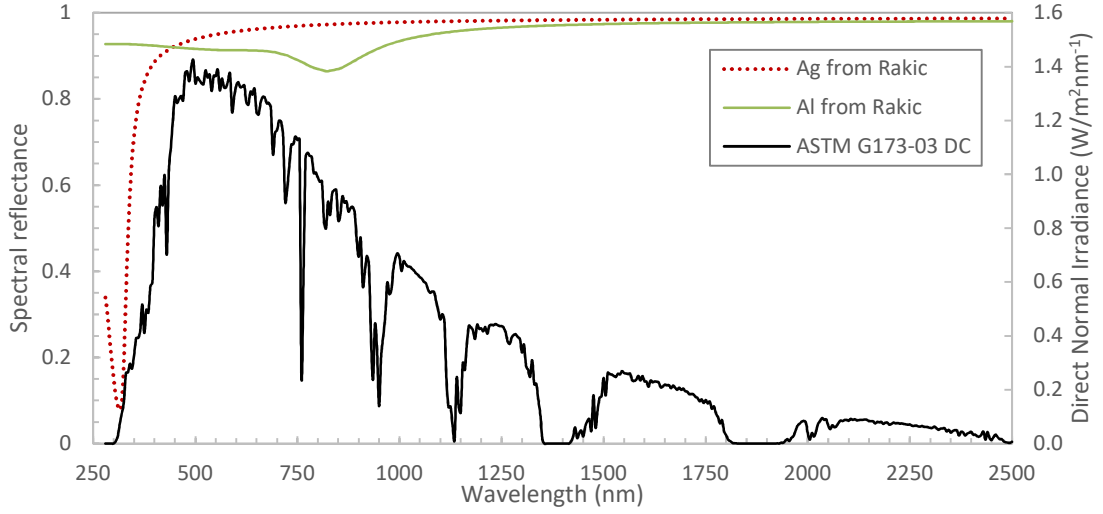


Figure 2 : Spectral reflectance over the solar domain (280 to 2500 nm) for Ag and Al substrates

### 3.2. Distributed Bragg Reflectors

In the introduction, we have pointed out that metallic layers are the simplest way to ensure high reflectance. Changing reflective properties involve changing complex refractive indices, which means changing the constitutive materials (chemical composition, crystallinity, surface roughness, etc.). This can be very complicated. Another way to ensure high reflectance is to use a Distributed Bragg Reflector (DBR) [50]. These reflectors allow reaching very high reflectance ( $R(\lambda) > 99\%$ ) at a specific wavelength  $\lambda$ . For this reason, they are critical components used in advanced optics applications such as lasers (vertical cavity surface emitting lasers, laser diodes, free electron lasers, fiber lasers, etc. [51–53]). To achieve this goal, the DBR uses a structure made of multiple bilayers of two different materials (noted 1 and 2) with varying refractive indices, repeated a high number of times. The total number of layers can be large, up to 20, or even more [50]. The thickness of each layer is adapted according to their refractive index. The maximum reflectance can be calculated using equation (2) [54], where:  $R(\lambda)$  is the reflectance at a specific wavelength  $\lambda$  at normal light incidence ( $0^\circ$ );  $Nb$  is the number of times the two different materials are repeated;  $n_1$  and  $n_2$  are the refractive indices of the two materials;  $n_0$  is the ambient refractive index;  $n_s$  is the substrate refractive index.

$$R(\lambda) = \left[ \frac{n_0(\lambda) \cdot n_2(\lambda)^{2Nb} - n_s(\lambda) \cdot n_1(\lambda)^{2Nb}}{n_0(\lambda) \cdot n_2(\lambda)^{2Nb} + n_s(\lambda) \cdot n_1(\lambda)^{2Nb}} \right]^2 \quad (2)$$

In air ( $n_0 = 1$ ) or even in glass ( $n_0 \approx 1.5$ ) it is possible to reach very high reflectance, up to 99%, by applying a high number of periods  $Nb$ , but only at a specific wavelength  $\lambda$ . With lower  $Nb$ , high reflectance can be obtained in a frequency/wavelength bandwidth  $\Delta\lambda$ . The latter can be estimated by equation (3) [54], where  $n_1$  and  $n_2$  are taken at the same chosen wavelength  $\lambda_i$ , and provided that  $n_1$  and  $n_2$  do not vary significantly with wavelength. The higher the difference between  $n_1$  and  $n_2$ , the larger the bandwidth.

$$\Delta\lambda(\lambda_i) = \frac{4}{\pi} \cdot \arcsin \left( \frac{n_2(\lambda_i) - n_1(\lambda_i)}{n_2(\lambda_i) + n_1(\lambda_i)} \right) \quad (3)$$

Applying DBRs to solar energy materials is however problematic due to the low value of  $\Delta\lambda$  attainable with known materials. Indeed, even when using (semi-)transparent materials with the lowest refractive indices (e.g.  $\text{MgF}_2$ ,  $n = 1.32$  at 587.6 nm) combined with the ones having the highest refractive indices (e.g. GaAs,  $n = 3.94$  at 587.6 nm), the bandwidth obtained is only around 380 nm, i.e., approximately 17% of the solar spectrum between 280 and 2500 nm. Figure 3 gives a graphical representation of the spectral reflectance of such DBR with 10 periods, supposing that the two materials are perfectly transparent ( $k = 0$  at all wavelengths). In reality GaAs is not, and absorbs part of the incident light, which reduces the maximum reflectance but does not impact the value of  $\Delta\lambda$ . If spectral reflectance (dotted red line) is higher than 99.99% from 475 to 800 nm, the corresponding solar reflectance is only close to 75%. It is around 20% less than a classical metallic mirror. The poor solar reflectance is due to the “sinusoidal” shape of the spectral reflectance on both sides of the frequency bandwidth. For this reason, DBRs are not suitable for concentrated solar applications. In contrast, they can be used in PV because the cell bandwidth can be reduced to the material band gap.

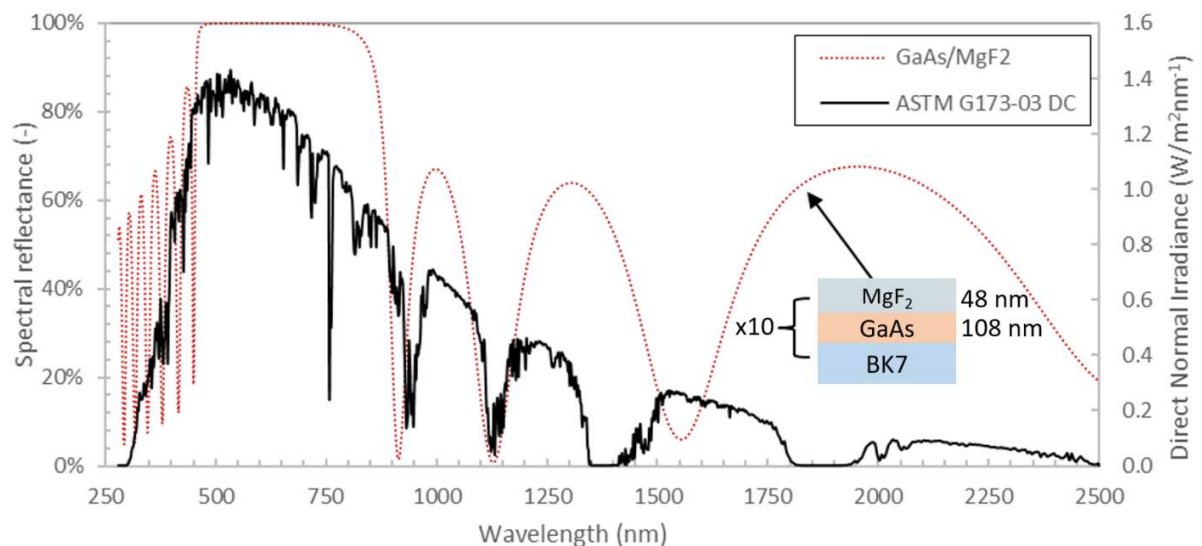


Figure 3 : Spectral reflectance over the solar domain (280 - 2500 nm) of a DBR made of 10  $\text{MgF}_2/\text{GaAs}$  bilayers on BK7 glass

### 3.3. Alternation of two materials on a metallic substrate

To improve the solar reflectance of metallic mirrors, we have tested structures inspired by DBRs: a couple of thin layers deposited several times on a substrate, as presented in Figure 4. Similarly to a DBR, the two constitutive materials ( $n^{\circ 1}$  and  $n^{\circ 2}$ ) have a large difference of complex refractive indices (noted respectively  $N_1$  and  $N_2$ ). In the following, the couples of two materials will be noted joined by a slash ("material 1 / material 2") in such specific order that Layer 1, i.e., the bottom layer of the bilayer, is made of material 1 and Layer 2, i.e., the top layer of the bilayer, is made of material 2 (Figure 4). The number of repetitions of these bilayers is noted  $Nb$ . The main difference with a DBR is that the stack is no longer periodic: each layer must have a specific thickness (noted  $d_i$ ), which is optimized to reach the highest solar reflectance possible, using the optimization method presented in section 3.2.

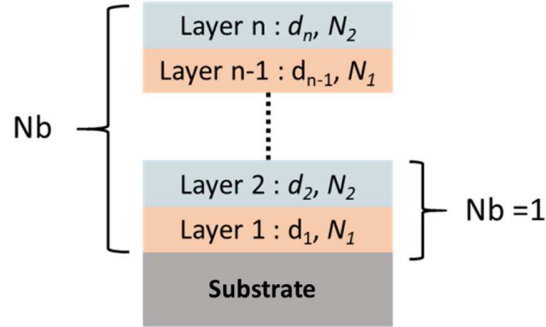


Figure 4 : Schematic representation of the alternation of two materials (thickness  $d$ , complex refractive index  $N$ ) on a substrate, with  $Nb$  the number of bilayers

Many combinations of two materials were tested and only the most relevant are presented in Table 1. The number of bilayers in the stack ( $Nb$ ) was fixed at 4 (for a total of 8 layers). This number was chosen with the idea of conserving stacks with a reasonable number of layers, for simpler simulation and potential fabrication, while still being able to observe the beneficial effect of the layers on the stack solar reflectance  $R_s$ . The gain in solar reflectance is calculated as compared to the metallic layer (Ag or Al) alone. The couples of materials are arranged by decreasing refractive index gradient  $n_2 - n_1$  between the two materials at 587.6 nm. When  $n_2 - n_1 > 0$  the material with the highest refractive index is on top of the bilayer. When  $n_2 - n_1 < 0$  the material with the lowest refractive index is on top.

Table 1 : Solar reflectance  $R_s$  of 8 dielectric layers ( $Nb = 4$ ) deposited on Ag and Al substrates. Each layer thickness was optimized to reach the highest solar reflectance.

|                                  | Material 1                | Material 2                | Refractive index gradient $n_2 - n_1$ | Ag substrate |               | Al substrate |               |
|----------------------------------|---------------------------|---------------------------|---------------------------------------|--------------|---------------|--------------|---------------|
|                                  |                           |                           |                                       | $R_s$        | $R_s$ gain    | $R_s$        | $R_s$ gain    |
| Metal alone                      | -                         | -                         | -                                     | 95.5%        | -             | 92.2%        | -             |
| Material with highest $n$ on top | $MgF_2$                   | $GaAs$                    | 2.57                                  | 85.2%        | - 10.3%       | 85.0%        | - 7.2%        |
|                                  | <b><math>MgF_2</math></b> | <b><math>TiO_2</math></b> | 1.03                                  | <b>97.6%</b> | <b>+ 2.1%</b> | <b>96.1%</b> | <b>+ 3.9%</b> |
|                                  | $SiO_2$                   | $TiO_2$                   | 0.94                                  | <b>97.2%</b> | <b>+ 1.7%</b> | <b>95.4%</b> | <b>+ 3.2%</b> |
|                                  | $MgF_2$                   | $ZrO_2$                   | 0.78                                  | 96.6%        | + 1.1%        | 94.4%        | + 2.2%        |
|                                  | $MgF_2$                   | $ZnO$                     | 0.63                                  | 96.3%        | + 0.8%        | 93.5%        | + 1.3%        |
|                                  | $MgF_2$                   | $SiO_2$                   | 0.13                                  | 94.8%        | - 0.7%        | 90.4%        | - 1.8%        |
| Material with lowest $n$ on top  | $SiO_2$                   | $MgF_2$                   | - 0.13                                | 94.8%        | - 0.7%        | 90.3%        | - 1.9%        |
|                                  | $ZnO$                     | $MgF_2$                   | - 0.63                                | 95.9%        | + 0.4%        | 93.1%        | + 0.9%        |
|                                  | $ZrO_2$                   | $MgF_2$                   | - 0.78                                | 96.1%        | + 0.6%        | 93.8%        | + 1.5%        |
|                                  | $TiO_2$                   | $SiO_2$                   | - 0.94                                | 96.4%        | + 0.9%        | 94.3%        | + 2.1%        |
|                                  | $TiO_2$                   | $MgF_2$                   | - 1.03                                | 96.5%        | + 1.0%        | 94.7%        | + 2.5%        |
|                                  | $GaAs$                    | $MgF_2$                   | - 2.57                                | 84.5%        | - 11.0%       | 83.7%        | - 8.5%        |

It can be observed in Table 1 that for the same couple of materials, it is more efficient to finish the stack (last layer in contact with air) with the material of highest refractive index. As an example,  $SiO_2/TiO_2$  gives a higher solar reflectance (97.2% on Ag) than  $TiO_2/SiO_2$  (96.4%). This is due to the higher refractive index gradient between the ambient medium (air,  $n_0 = 1$ ) and the first (top) layer met by the incident light. The more refractive the top layer, the more incident

solar power is refracted by the air-top layer interface, i.e., the more power enters the stack, and can then get reflected back by the mirror. From this point of view, such a stack can be considered to act as an “antireflective coating” for reflective layers.

The highest gain in solar reflectance is obtained with MgF<sub>2</sub>/TiO<sub>2</sub> bilayers, for both Ag and Al substrates. The refractive index gradient between these two materials,  $n_2 - n_1 = 1.03$ , is the second highest after MgF<sub>2</sub>/GaAs ( $n = 2.41$  for TiO<sub>2</sub>,  $n = 1.38$  for MgF<sub>2</sub>, both at 587.6 nm). For Ag, solar reflectance increases from 95.5% to 97.6 % (+ 2.1%). Noticeably, for Al solar reflectance even jumps from 92.2% to 96.1% (+ 3.9%), which means that such Al/MgF<sub>2</sub>/TiO<sub>2</sub> mirror has a higher solar reflectance than Ag reflectors (95.5%). These two materials are a suitable and realistic choice, since they are commonly used in industry and are the subject of hundreds of publications. MgF<sub>2</sub> is indeed a well-known antireflective coating, particularly for glass. It is also used in lenses or laser industries [55]. TiO<sub>2</sub> is also cited as antireflective coating and provides self-cleaning effect [56]. It is also used in photocatalytic applications as nanoparticles or as a white pigment [57].

Very interesting results are also obtained with SiO<sub>2</sub>/TiO<sub>2</sub> stacks. Here SiO<sub>2</sub> replaces MgF<sub>2</sub> as lowest refractive index material in the stack. SiO<sub>2</sub> has a higher refractive than MgF<sub>2</sub> ( $n = 1.47$  vs.  $n = 1.38$ , at 587.6 nm) but the refractive index gradient with TiO<sub>2</sub> is still high (0.94). Even though it is less efficient, this replacement can reduce fabrication costs, due to the maturity of deposition techniques and the cost of precursor materials. Indeed the fabrication of SiO<sub>2</sub> is currently cheaper than that of MgF<sub>2</sub>, and SiO<sub>2</sub> can easily be deposited by sol-gel techniques, as shown by an impressive quantity of papers [58], [59]. Moreover, the solar reflectance gain is still quite noticeable with SiO<sub>2</sub>/TiO<sub>2</sub>: +1.7% for Ag and +3.2% for Al. For Al,  $R_s$  can reach 95.4%, which is very close (0.1%) to the natural solar reflectance of Ag alone (95.5%). This improvement demonstrates that the systematic utilization of silver for CSP mirrors could be replaced by using low cost materials, Al, SiO<sub>2</sub> and TiO<sub>2</sub>, deposited by similar and well-known fabrication techniques.

Overall, a high refractive index gradient  $|n_2 - n_1|$  between the two materials is key to increasing solar reflectance, as shown by results obtained with all couples in Table 1, with the notable exception of GaAs. Indeed, GaAs coupled with MgF<sub>2</sub> leads to the worst results, with the lowest solar reflectance of 85.2% despite the highest refractive index gradient of 2.57 ( $n = 3.95$  vs.  $n = 1.38$  at 587.6 nm). It can be explained by the relatively high solar absorption of GaAs (42% at 1000 nm, see Figure 1) compared to that of the other considered materials (MgF<sub>2</sub>, SiO<sub>2</sub>, ZnO, ZrO<sub>2</sub>, TiO<sub>2</sub>) for which the absorption is very low, below 0.1% at 1000 nm. The real part  $n$  of the refractive index cannot be the only criterion to select dielectric materials for solar mirrors. Their transparency in the solar range is also paramount, especially for high  $Nb$  values.

### 3.4. MgF<sub>2</sub>/TiO<sub>2</sub> and SiO<sub>2</sub>/TiO<sub>2</sub> optimized stacks

This section details the results obtained with MgF<sub>2</sub>/TiO<sub>2</sub> and SiO<sub>2</sub>/TiO<sub>2</sub> 8-layer stacks on Ag and Al substrates, as they give the highest gains in solar reflectance. Figure 5 illustrates MgF<sub>2</sub>/TiO<sub>2</sub> optimized stacks with optimal layer thicknesses, depending on the considered substrate. No very thin layer (< 20 nm) is required. The deposition of very thin layers is difficult to control, and because of the low number of atoms, their optical properties can be different than

thicker layers. Also, the tolerance on thickness errors for these structures is high: a simulated error of  $\pm 10$  nm on each of the 8 layers was found to reduce the solar reflectance by less than 0.5% (in absolute scale).

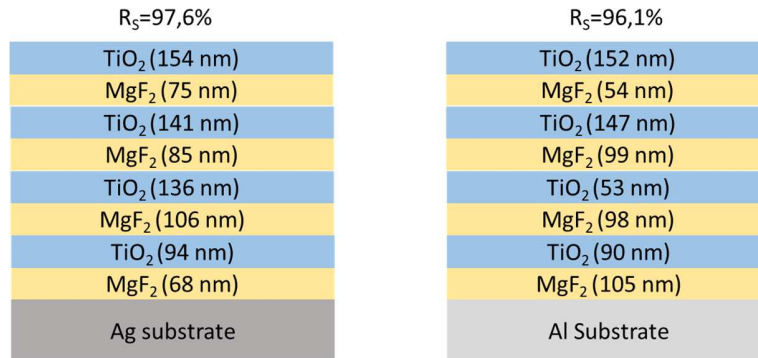


Figure 5 : Optimized  $\text{MgF}_2/\text{TiO}_2$  8-layer coatings for solar mirrors using Al and Ag reflectors

The optimized stacks presented in Figure 5 are the best solution, but not the only available. Different runs of the optimization process gave different optimized stacks with very close solar reflectance (difference  $\leq -0.1\%$ ), but rather different layer thicknesses. Table 2 presents two alternative results for each substrate.

Table 2 : Alternative layer thicknesses for optimized  $\text{MgF}_2/\text{TiO}_2$  8-layer stacks

| Substrate | $R_s$ | Layer 1 | Layer 2 | Layer 3 | Layer 4 | Layer 5 | Layer 6 | Layer 7 | Layer 8 | Total  |
|-----------|-------|---------|---------|---------|---------|---------|---------|---------|---------|--------|
| Ag        | 97.5% | 84 nm   | 95 nm   | 85 nm   | 61 nm   | 106 nm  | 144 nm  | 73 nm   | 76 nm   | 723 nm |
| Ag        | 97.5% | 72 nm   | 71 nm   | 79 nm   | 106 nm  | 87 nm   | 116 nm  | 105 nm  | 165 nm  | 802 nm |
| Al        | 96.0% | 106 nm  | 107 nm  | 98 nm   | 70 nm   | 82 nm   | 89 nm   | 69 nm   | 171 nm  | 792 nm |
| Al        | 96.0% | 79 nm   | 63 nm   | 133 nm  | 51 nm   | 155 nm  | 105 nm  | 167 nm  | 103 nm  | 855 nm |

Figure 6 represents the spectral reflectance of the two optimized stacks shown in Figure 5. The global aspect of these spectra is very different than that of metallic reflectors (Figure 2). Several quick drops in spectral reflectance are visible. They result from destructive interference at specific wavelengths (antireflection effect). It can be noted that some of these reflectance drops (e.g. at 900 nm for Al and 1100 nm for Ag) coincide with low solar direct normal irradiance (at 950 nm and 1130 nm). This illustrates the pertinence of the optimization.

Also, the reflective properties in the UV domain (280 - 400 nm) are notably modified by the  $\text{MgF}_2/\text{TiO}_2$  stack. Ag and Al respectively reflect 74.8% (i.e., absorb 25.2%) and 92.5% of the UV flux density, whereas the  $\text{MgF}_2/\text{TiO}_2$ -coated Ag and Al mirrors reflect 87.4% (i.e., absorb 12.6%) and 91% of the same. Moreover, UV photons cause major degradation to solar mirrors, especially on the protective paints behind the metallic reflector. According to the conservation of energy, as the metallic substrate is opaque, every photon not reflected is absorbed. Dividing by two (12.6% vs. 25.2%) the UV flux absorbed by the silver-based mirror (by increasing its reflectance in this domain) can have a positive impact on its durability [7].

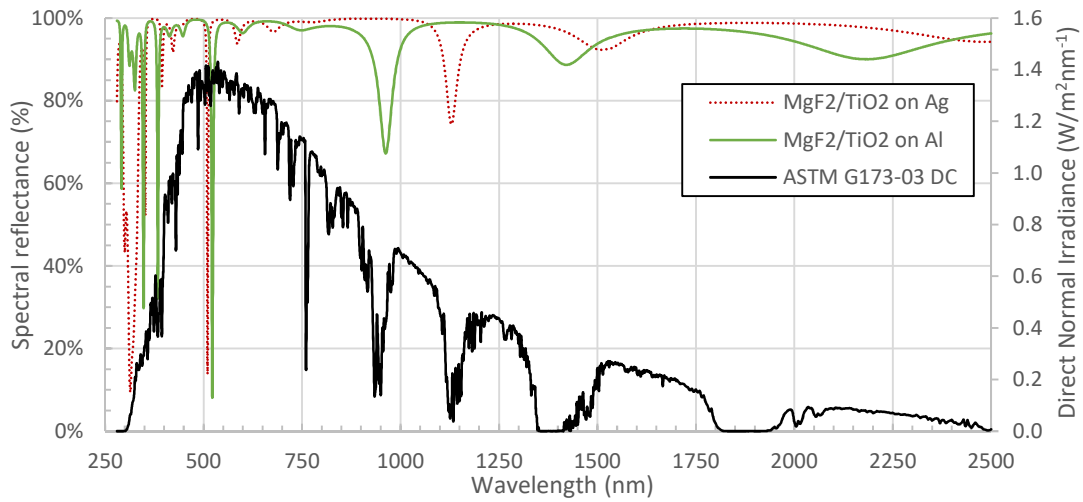


Figure 6 : Spectral reflectance of MgF<sub>2</sub>/TiO<sub>2</sub> optimized 8-layer stacks on Al and Ag substrates

Since SiO<sub>2</sub>/TiO<sub>2</sub> stacks are a lower cost alternative to MgF<sub>2</sub>/TiO<sub>2</sub> ones, although they have lower performance, SiO<sub>2</sub>/TiO<sub>2</sub> optimized stacks are also illustrated in Figure 7, while their specular reflectance is illustrated in Figure 8. The same observations can be made in this case.

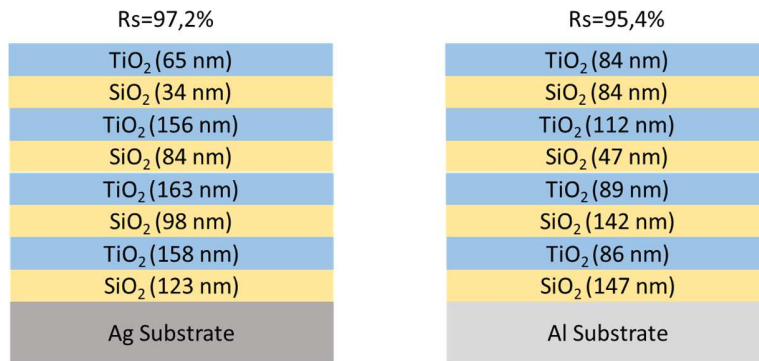


Figure 7 : Optimized SiO<sub>2</sub>/TiO<sub>2</sub> 8-layer coatings for solar mirrors using Al and Ag reflectors

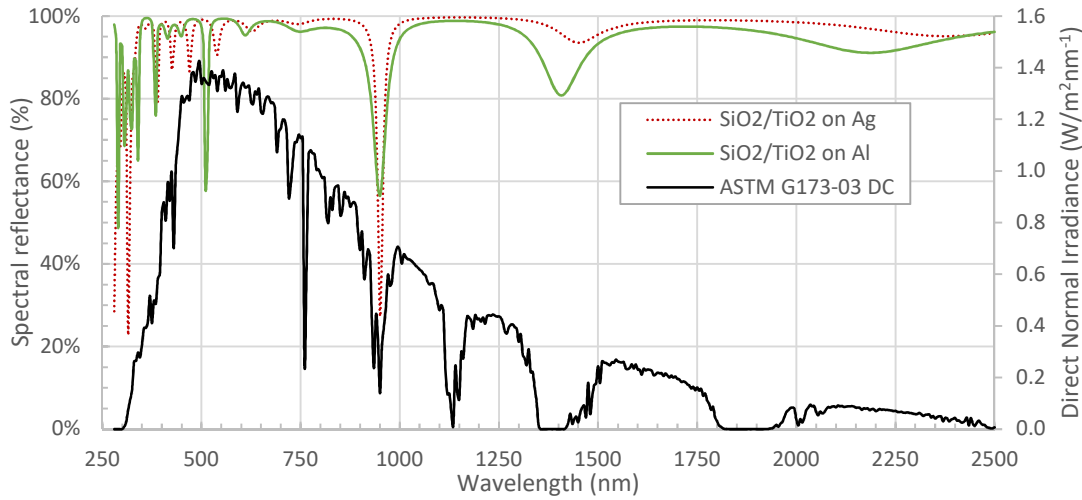


Figure 8 : Spectral reflectance for SiO<sub>2</sub>/TiO<sub>2</sub> optimized 8-layer stacks on Al and Ag substrates

### 3.5. Impact of light angle of incidence

All previous results were obtained by considering the sunlight angle of incidence (AOI) to be normal (0°) to the surface of the mirror, which is unrealistic compared to operational conditions. Indeed many factors cause an angular distribution ( $\neq 0^\circ$ ) of the solar irradiance seen by the mirror: imperfect sun tracking, cosine effect, the concentrator geometric form, etc. Solar reflectance was therefore also calculated for several AOIs.

Figure 9 shows the solar reflectance vs. AOI, for simple Ag and Al mirrors (dotted lines) and for the same metals with additional MgF<sub>2</sub>/TiO<sub>2</sub> stacks ( $Nb = 4, 8$  layers, solid lines). These stacks are the ones optimized for an AOI of 0° (section 3.4). For all mirrors, increasing the AOI tends to decrease the solar reflectance. The AOI however has little effect on the solar reflectance of Ag-based mirrors (red lines). Indeed, the maximum loss in  $R_S$  is observed at AOI = 70° is -0.2% for a simple Ag mirror and -0.7% for Ag mirror with MgF<sub>2</sub>/TiO<sub>2</sub> coating. Al-based mirrors (green lines) are more sensitive to the AOI, as shown by the curves decrease, especially for AOI > 40°. The simple Al mirror suffers a loss of 3.2% in solar reflectance between AOI = 0° and AOI = 70°, while Al + MgF<sub>2</sub>/TiO<sub>2</sub> stack loses 2.9%. In any case, whatever the angle of incidence, the additional MgF<sub>2</sub>/TiO<sub>2</sub> stack has a positive effect on the solar reflectance of the metal (Ag and Al).

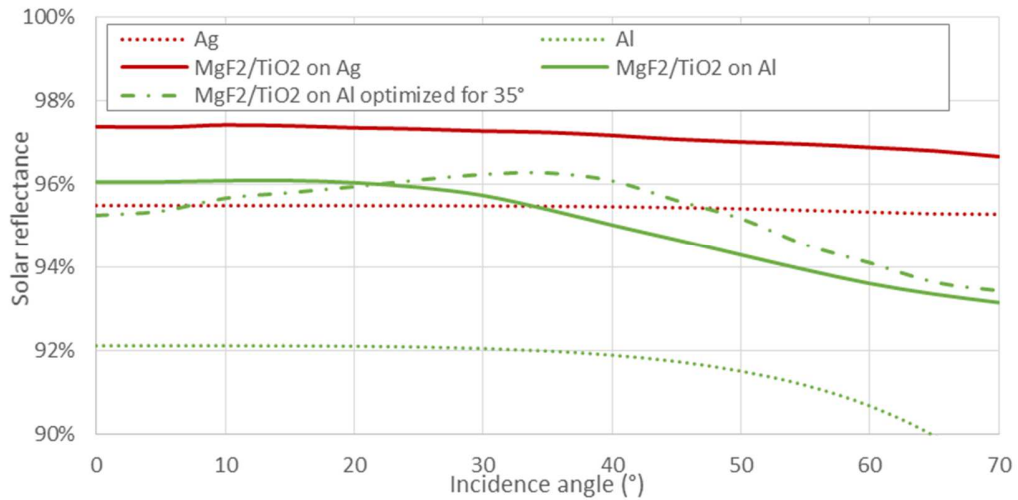


Figure 9 : Solar reflectance of mirrors vs. light angle of incidence (AOI)

As observed for the previous optimizations at  $0^\circ$ , an Al mirror with  $\text{MgF}_2/\text{TiO}_2$  top coating (solid green line) is more efficient than a simple Ag mirror (dotted red line). However due to the low sensitivity to AOI of Ag solar reflectance, this remains true only for low AOIs  $< 35^\circ$ . Above  $40^\circ$ , the Ag mirror becomes more efficient again.

To suitably choose the best mirror for CSP applications, the knowledge of the annual AOI distribution in the solar field is therefore necessary. This distribution results from the complex interaction of the plant location and the collector geometry. As a reference, Sutter et al. [60] have calculated typical annual angle distributions for four locations (from Equator to Plataforma Solar de Almeria solar plants in Southeast Spain) and two different technologies: Parabolic Trough Collector (PTC) and solar tower. They have found that the mean annual AOI varies from  $27.8^\circ$  to  $34.8^\circ$ . This tends to indicate that our Al +  $\text{MgF}_2/\text{TiO}_2$  solution can still be the best option over Ag.

Moreover, the stacks presented so far were optimized for a normal incidence. To better adapt to the abovementioned mean annual AOI, the  $\text{MgF}_2/\text{TiO}_2$  stack was thus also optimized for AOI =  $35^\circ$  (dashed green line in Figure 9). This Al +  $\text{MgF}_2/\text{TiO}_2$  mirror optimized for  $35^\circ$  is more efficient than Ag for AOI between  $8^\circ$  and  $47^\circ$ , with a maximum gain in  $R_S$  of 0.8% at  $35^\circ$  compared to Ag alone.

In addition, the average solar reflectance  $R_S$  over one year was calculated for these five solar mirrors (Ag and Al alone, Ag and Al with  $\text{MgF}_2/\text{TiO}_2$  stack optimized for AOI =  $0^\circ$ , Al +  $\text{MgF}_2/\text{TiO}_2$  optimized for AOI =  $35^\circ$ ). For this purpose, the AOI annual distributions from [60] for five different sites were used. Table 3 presents the results, where PSA\* is a solar tower heliostat field at the Plataforma Solar de Almeria (PSA) in Spain and the four other sites are parabolic trough solar fields. The values of solar reflectance at normal incidence (Table 1) are also recalled as a comparison.

When considering these annual averages, Al and Ag mirrors have standard performance, just slightly lower than at normal incidence. Adding an  $\text{MgF}_2/\text{TiO}_2$  optimized stack on Ag or Al still increases their performance, but not as much as when just considering normal incidence. As a consequence, the performance of Al +  $\text{MgF}_2/\text{TiO}_2$  (optimized for AOI =  $0^\circ$ ) becomes inferior or

equivalent to that of Ag alone: if  $R_S$  was 96.1% at AOI = 0°, it is comprised between 94.7% and 95.6% when considering the annual average. In this case substituting Ag by Al + MgF<sub>2</sub>/TiO<sub>2</sub> is not efficient in terms of solar reflectance. Contrarily, the mirror made of Al with MgF<sub>2</sub>/TiO<sub>2</sub> stack optimized for 35° is not only more efficient than the one optimized for 0° (+0.3-0.5%) but also more performing than the simple Ag mirror (except for PSA\*). The use of an additional dielectric stack, optimized for an average incidence angle, above a metal reflector, is thus an efficient solution to tune and maximize the solar performance of CSP mirrors for their region of implantation and type of collector.

Table 3 : Average solar reflectance  $R_S$  of mirrors for five locations considering annual AOI distribution [60]

| Mirror                                  | Angle of Optimization | Average $R_S$ with annual AOI distribution |            |       |         |       | AOI = 0° (Table 1) |
|---|-----------------------|--|------------|-------|---------|-------|--------------------|
|   |                       | PSA  | Ouarzazate | Aswan | Equator | PSA*  |                    |
| Ag alone                                | -                     | 95.5%                                      | 95.5%      | 95.5% | 95.5%   | 95.3% | 95.5%              |
| Ag + MgF <sub>2</sub> /TiO <sub>2</sub> | 0°                    | 97.2%                                      | 97.2%      | 97.2% | 97.3%   | 96.4% | 97.6%              |
| Al alone                                | -                     | 91.8%                                      | 91.9%      | 91.9% | 92.0%   | 91.1% | 92.2%              |
| Al + MgF <sub>2</sub> /TiO <sub>2</sub> | 0°                    | 95.2%                                      | 95.3%      | 95.4% | 95.6%   | 94.7% | 96.1%              |
| Al + MgF <sub>2</sub> /TiO <sub>2</sub> | 35°                   | 95.7%                                      | 95.8%      | 95.9% | 96.0%   | 95.0% | 95.9%              |

### 3.6. Impact of the number of layers

All results with dielectric stacks presented above were obtained with a total of eight dielectric layers ( $Nb = 4$ ). This number was chosen as a compromise between a reasonable number of layers to simulate/optimize (i.e., a reasonable calculation time) and eventually to fabricate, and a significant gain in solar performance. Since the most promising material combination was identified as MgF<sub>2</sub>/TiO<sub>2</sub>, the impact of the number of layers on solar performance can now be studied. For this purpose, let us consider the solar reflectance of Ag and Al substrates with a varying number  $Nb$  of MgF<sub>2</sub>/TiO<sub>2</sub> dielectric top layers, simulated and optimized for normal incidence. The results are presented in Figure 10 for  $Nb = 1$  to 10, i.e., 2 to 20 layers in total.

For a given number of layers, the best results are always obtained with Ag substrate (in red). The gap between the solar reflectance of Ag and Al however decreases when the number of MgF<sub>2</sub>/TiO<sub>2</sub> layers increases: 3.3% for metal alone, 1.4% for 10 layers and only 0.4% for 20 layers. It is found possible to exceed 98.0% of solar reflectance with 12 layers or more for Ag substrate, and with 18 layers or more with Al substrate.

The gain in solar reflectance with adding dielectric layers is not linear. The first two layers provide a solar reflectance improvement of +0.9% for Ag and + 2.15% for Al, while changing the number of layers from 18 to 20 only improves  $R_S$  by + 0.1% in both cases. Thus there is an optimal number of layers that gives the best compromise between the additional cost of these layers (in terms of additional deposition time and materials, e.g., PVD targets and sol-gel precursors) and the corresponding improvement in solar performance.

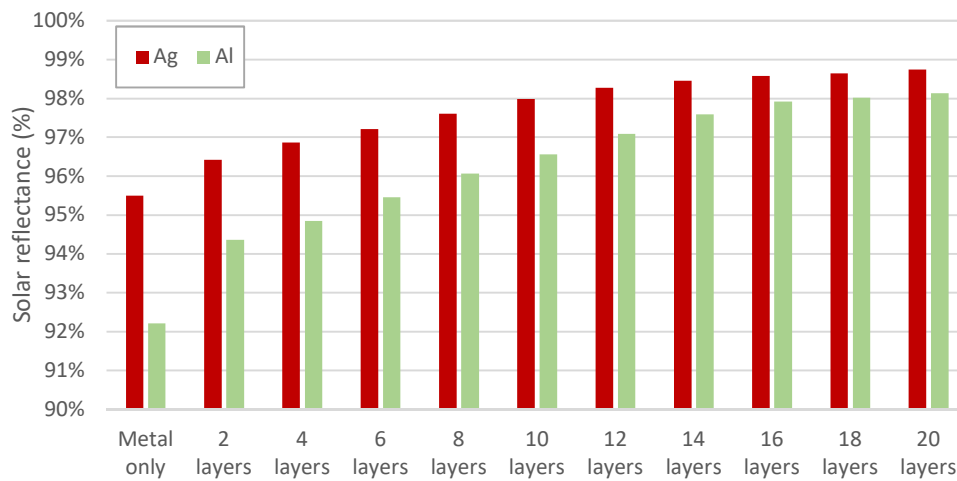


Figure 10 : Solar reflectance of Ag or Al substrates with optimized  $\text{MgF}_2/\text{TiO}_2$  stack vs. total number of layers in the stack

### 3.7. Complete mirror

For metallic mirrors used as reflectors in solar energy applications, durability is a critical issue [12]. Researchers and industrials commonly cite the objective of 20 years of operation without major degradation (i.e., solar reflectance loss above 5%). Current silvered glass mirrors achieve this goal. To be competitive, our solution of metal reflectors with dielectric top layers must reach this goal as well. Reflective layers on current solar mirrors are actually protected on both sides: on the back side with an anticorrosion protective layer (e.g. a thin copper layer) and polymer paints, and on the front side with 1 to 4 mm of glass. For our mirrors, these technical solutions are also conceivable. The utilization of protective layers above the dielectric layers do not affect the solar reflectance improvement. On the backside, the utilization of paints has no more influence than for current mirrors. We can easily imagine an inverse deposition process, as is done for current mirrors: first depositing the dielectric layers on a glass substrate (the material with higher refractive index being deposited first), then depositing the metallic reflector (100 - 150 nm of Ag or Al), and finally applying a protective layer and the backside paints. The suggested architecture is illustrated in Figure 11.

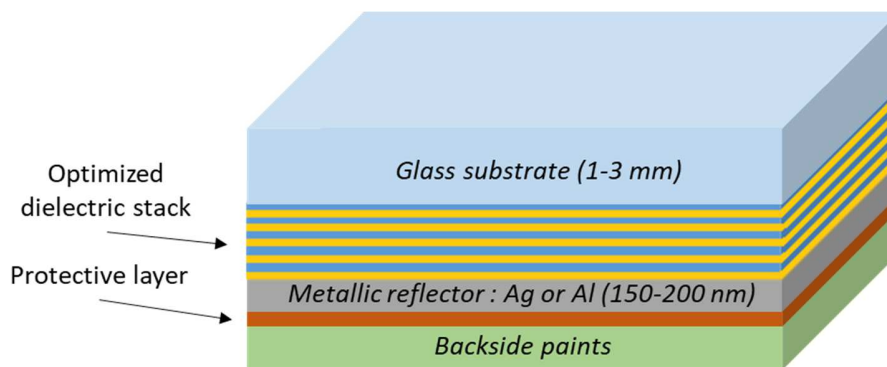


Figure 11 : Suggested complete mirror with metallic reflector (Ag or Al) and optimized dielectric stack on a glass substrate

#### 4. CONCLUSION

A large majority of solar mirrors used in commercial concentrated solar plants is made of a thin silver reflector layer ( $< 200$  nm) between glass and paints, to ensure a high reflectance in all the solar spectrum, with a high durability over decades. Even though silver is a very good solar reflector, the worldwide reserve of this metal is finite and the risk of silver shortage is real.

Considering this, optical simulations and optimizations were carried out, to explore the possibilities of reaching high solar reflectance above 95%, without having recourse to silver. This objective was achieved by adding thin dielectric bilayers of  $\text{MgF}_2/\text{TiO}_2$  on an aluminum reflector. This structure was inspired by Distributed Bragg Reflectors, only in this case all layer thicknesses were separately optimized instead of fixed. The solar reflectance of an optimized  $[\text{Al} + (\text{MgF}_2/\text{TiO}_2) \times 4]$  mirror is expected to be 96.1 %, higher than a silver reflector (95.5%), without using any rare materials. Other dielectric couples, such as  $\text{SiO}_2/\text{TiO}_2$ , can also generate a similar gain in reflectance, with the additional advantage to use low cost materials. In addition, the dielectric stack can be optimized according to a specific distribution of light incidence angles, to render the mirror even more efficient at a specific location and/or for a specific CSP technology/collector type. These findings allow us to imagine a future where silver supply for CSP is a lesser issue. Furthermore, with these dielectric stacks, it is also possible to render the existing silver mirrors even more reflective, with a solar reflectance of 97.5% for four  $\text{MgF}_2/\text{TiO}_2$  bilayers, thus allowing to collect more solar energy (and produce more heat and electricity) with the same amount of silver.

#### 5. ACKNOWLEDGMENTS AND FUNDING

This work was supported by the French "Investments for the future" program managed by the National Agency for Research under contract ANR-10-LABX-22-01-SOLSTICE. The authors would like to thank Florian Sutter from DLR for providing incidence angle distribution charts.

#### 6. REFERENCES

- [1] E. Panos, M. Densing, K. Volkart, Access to electricity in the World Energy Council's global energy scenarios: An outlook for developing regions until 2030, Energy Strategy Reviews. 9 (2016) 28–49. <https://doi.org/10.1016/j.esr.2015.11.003>.

- [2] R.L. Moss, E. Tzimas, H. Kara, P. Willis, J. Kooroshy, *Critical Metals in Strategic Energy Technologies*, 2011. <https://doi.org/10.2790/35600>.
- [3] Silver Institute, (2020). <https://www.silverinstitute.org> (accessed May 18, 2019).
- [4] E. Bellini, *PV Magazine*, (2019). <https://www.pv-magazine.com> (accessed April 5, 2019).
- [5] C.E. Kennedy, K. Terwilliger, Optical Durability of Candidate Solar Reflectors, *Journal of Solar Energy Engineering*. 127 (2005) 262. <https://doi.org/10.1115/1.1861926>.
- [6] T. Fend, B. Hoffschmidt, G. Jorgensen, H. Küster, D. Krüger, R. Pitz-Paal, P. Rietbrock, K.J. Riffelmann, Comparative assessment of solar concentrator materials, *Solar Energy*. 74 (2003) 149–155. [https://doi.org/10.1016/S0038-092X\(03\)00116-6](https://doi.org/10.1016/S0038-092X(03)00116-6).
- [7] C. Avenel, O. Raccurt, J.-L. Gardette, S. Therias, Accelerated aging test modeling applied to solar mirrors, *Npj Materials Degradation*. 3 (2019) 1–14. <https://doi.org/10.1038/s41529-019-0089-y>.
- [8] C.K. Ho, J. Sment, J. Yuan, C.A. Sims, Evaluation of a reflective polymer film for heliostats, *Solar Energy*. 95 (2013) 229–236. <https://doi.org/10.1016/j.solener.2013.06.015>.
- [9] A.W. Czanderna, P. Schissel, Specularity and stability of silvered polymers, *Solar Energy Materials*. 14 (1986) 341–356. [https://doi.org/10.1016/0165-1633\(86\)90057-2](https://doi.org/10.1016/0165-1633(86)90057-2).
- [10] C.E. Kennedy, K. Terwilliger, Optical Durability of Candidate Solar Reflectors, *Journal of Solar Energy Engineering*. 127 (2005) 262. <https://doi.org/10.1115/1.1861926>.
- [11] P. Karasiński, J. Jaglarz, M. Reben, E. Skoczek, J. Mazur, Porous silica xerogel films as antireflective coatings - Fabrication and characterization, *Optical Materials*. 33 (2011) 1989–1994. <https://doi.org/10.1016/j.optmat.2011.04.003>.
- [12] C. Avenel, O. Raccurt, J.L. Gardette, S. Therias, Review of accelerated ageing test modelling and its application to solar mirrors, *Solar Energy Materials and Solar Cells*. 186 (2018) 29–41. <https://doi.org/10.1016/j.solmat.2018.06.024>.
- [13] X. Liang, S. Luan, Z. Yin, M. He, C. He, L. Yin, Y. Zou, Z. Yuan, L. Li, X. Song, C. Lv, W. Zhang, Recent advances in the medical use of silver complex, *European Journal of Medicinal Chemistry*. 157 (2018) 62–80. <https://doi.org/10.1016/j.ejmech.2018.07.057>.
- [14] M. Ahamed, M.S. AlSalhi, M.K.J. Siddiqui, Silver nanoparticle applications and human health, *Clinica Chimica Acta*. 411 (2010) 1841–1848. <https://doi.org/10.1016/j.cca.2010.08.016>.
- [15] D.J. Barillo, D.E. Marx, Silver in medicine: A brief history BC 335 to present, *Burns*. 40 (2014) S3–S8. <https://doi.org/10.1016/j.burns.2014.09.009>.
- [16] W. Smith, *A dictionary of Greek and Roman Antiquities*, London, 1859.
- [17] P. Fayet, F. Granzer, G. Hegenbart, E. Moisar, B. Pischel, L. Wöste, The role of small silver clusters in photography, *Zeitschrift Für Physik D Atoms, Molecules and Clusters*. 3 (1986) 299–302. <https://doi.org/10.1007/BF01384819>.
- [18] R. O’Connell, A. Cameron, A. Bruce, S. Litosh, S. Nambiath, J. Wiebe, W. Yao, K. Norton, S. Li, D. Aranda, N. Scott-Gray, Z. Chan, E. Balsamo, *World Silver Survey 2018*, 2018.
- [19] A. Laugharne, I. Yucel, *The Role of Silver in the Green Revolution Prepared for The Silver Institute*, 2018.
- [20] H.U. Sverdrup, D. Koca, K.V. Ragnarsdóttir, Peak Metals, Minerals, Energy, Wealth, Food and Population: Urgent Policy Considerations for a Sustainable Society, *Journal of Environmental Science and Engineering*. 2 (2013) 189–222.
- [21] S.M. Bennett, *Silver USGS 2018 Report*, U.S Geological Survey, Mineral Commodity Summaries. (2019) 150–151.

- [22] L. Grandell, A. Thorenz, Silver supply risk analysis for the solar sector, *Renewable Energy*. 69 (2014) 157–165. <https://doi.org/10.1016/j.renene.2014.03.032>.
- [23] A. García-Olivares, Substituting silver in solar photovoltaics is feasible and allows for decentralization in smart regional grids, *Environmental Innovation and Societal Transitions*. 17 (2015) 15–21. <https://doi.org/10.1016/j.eist.2015.05.004>.
- [24] G. Schubert, G. Beaucarne, J. Hoornstra, The future of metallization - Results from questionnaires of the four workshops from 2008 to 2013, *Energy Procedia*. 43 (2013) 12–17. <https://doi.org/10.1016/j.egypro.2013.11.083>.
- [25] Alanod Solar, (n.d.). <http://www.alanod-solar.com/de> (accessed August 20, 2015).
- [26] A. Grosjean, A. Soum-Glaude, P. Neveu, L. Thomas, Comprehensive simulation and optimization of porous SiO<sub>2</sub> antireflective coating to improve glass solar transmittance for solar energy applications, *Solar Energy Materials and Solar Cells*. 182 (2018) 166–177. <https://doi.org/10.1016/J.SOLMAT.2018.03.040>.
- [27] A. Soum-Glaude, I. Bousquet, L. Thomas, G. Flamant, Optical modeling of multilayered coatings based on SiC(N)H materials for their potential use as high-temperature solar selective absorbers, *Solar Energy Materials and Solar Cells*. 117 (2013) 315–323. <https://doi.org/10.1016/j.solmat.2013.06.030>.
- [28] D. Ngoue, A. Grosjean, L. Di Giacomo, S. Quozola, A. Soum-Glaude, L. Thomas, Y. Lalau, R. Reoyo-Prats, B. Claudet, O. Faugeroux, C. Leray, A. Toutant, J.-Y. Peroy, A. Ferrière, G. Olalde, Ceramics for concentrated solar power (CSP): From thermophysical properties to solar absorbers, *Advanced Ceramics for Energy Conversion and Storage*. (2020) 89–127. <https://doi.org/10.1016/B978-0-08-102726-4.00003-X>.
- [29] C.C. Katsidis, D.I. Siapkas, General transfer-matrix method for optical multilayer systems with coherent, partially coherent, and incoherent interference, *Applied Optics*. 41 (2002) 3978–3987. <https://doi.org/10.1364/AO.41.003978>.
- [30] L. Simonot, S. Mazauric, Matrix method to predict the spectral reflectance of stratified surfaces including thick layers and thin films, *HAL Archive*. (2015) 1–20.
- [31] Sh.A. Furman, A.V. Tikhonravov, *Basics of optics of multilayer systems*, Edition Fr, Gif-sur-Yvette, 1992.
- [32] S. Meyen, M. Montecchi, C. Kennedy, G. Zhu, Parameters and method to evaluate the solar reflectance properties of reflector materials for concentrating solar power technology, *SolarPACES*. (2013).
- [33] C.A. Gueymard, D. Myers, K. Emery, Proposed reference irradiance spectra for solar energy systems testing, *Solar Energy*. 73 (2002) 443–467. [https://doi.org/10.1016/S0038-092X\(03\)00005-7](https://doi.org/10.1016/S0038-092X(03)00005-7).
- [34] A. Fernández-García, F. Sutter, M. Montecchi, F. Sallaberry, A. Heimsath, C. Heras, E. Le Baron, A. Soum-Glaude, Parameters and method to evaluate the reflectance properties of reflector materials for concentrating solar power technology, *SolarPACES Official Reflectance Guideline Version 3.0*, (2018).
- [35] A. Heimsath, P. Nitz, Scattering and specular reflection of solar reflector materials – Measurements and method to determine solar weighted specular reflectance, *Solar Energy Materials and Solar Cells*. 203 (2019). <https://doi.org/10.1016/j.solmat.2019.110191>.
- [36] Scilab, *Scilab v5.5.0*, (n.d.).
- [37] J.H. Holland, *Adaptation in natural and artificial systems*, 1975.
- [38] J. Mouret, *Evolutionary Adaptation in Natural and Artificial Systems*, (2016).

- [39] A.D. Rakic, A.B. Djuricic, J.M. Elazar, M.L. Majewski, Optical properties of metallic films for vertical-cavity optoelectronic devices., *Applied Optics*. 37 (1998) 5271–5283. <https://doi.org/10.1364/AO.37.005271>.
- [40] M.J. Dodge, Refractive properties of magnesium fluoride, *Applied Optics*. 23 (1984) 1980. <https://doi.org/10.1364/AO.23.001980>.
- [41] L. Gao, F. Lemarchand, M. Lequime, Exploitation of multiple incidences spectrometric measurements for thin film reverse engineering., *Optics Express*. 20 (2012) 15734–51. <https://doi.org/10.1364/OE.20.015734>.
- [42] W.L. Bond, Measurement of the refractive indices of several crystals, *Journal of Applied Physics*. 36 (1965) 1674–1677. <https://doi.org/10.1063/1.1703106>.
- [43] D.L. Wood, K. Nassau, Refractive index of cubic zirconia stabilized with yttria, 21 (1982) 2978–2981.
- [44] T. Siefke, S. Kroker, K. Pfeiffer, O. Puffky, K. Dietrich, D. Franta, I. Ohlídal, A. Szeghalmi, E.B. Kley, A. Tünnermann, Materials Pushing the Application Limits of Wire Grid Polarizers further into the Deep Ultraviolet Spectral Range, *Advanced Optical Materials*. 4 (2016) 1780–1786. <https://doi.org/10.1002/adom.201600250>.
- [45] A.D. Rakić, M.L. Majewski, Modeling the optical dielectric function of GaAs and AlAs: Extension of Adachi’s model, *Journal of Applied Physics*. 80 (1996) 5909–5914. <https://doi.org/10.1063/1.363586>.
- [46] H.K. Pulker, H.K. Pulker, Application of Coatings on Glass, *Coatings on Glass*. (1999) 429–510. <https://doi.org/10.1016/B978-044450103-5/50012-1>.
- [47] C. Stelling, C.R. Singh, M. Karg, T.A.F. König, M. Thelakkat, M. Retsch, Plasmonic nanomeshes : their ambivalent role as transparent electrodes in organic solar cells, *Nature Publishing Group*. (2017) 1–13. <https://doi.org/10.1038/srep42530>.
- [48] I. Bodurov, I. Vlaeva, A. Viraneva, T. Yovcheva, S. Saino, Modified design of a laser refractometer, *Nanoscience & Nanotechnology*. 16 (2016) 31–33.
- [49] K.M. McPeak, S. V. Jayanti, S.J.P. Kress, S. Meyer, S. Iotti, A. Rossinelli, D.J. Norris, Plasmonic films can easily be better: Rules and recipes, *ACS Photonics*. 2 (2015) 326–333. <https://doi.org/10.1021/ph5004237>.
- [50] R. Jambunathan, J. Singh, Design studies for distributed Bragg reflectors for short-cavity edge-emitting lasers, *IEEE Journal of Quantum Electronics*. 33 (1997) 1180–1189. <https://doi.org/10.1109/3.594882>.
- [51] P. Good, T. Cooper, M. Querci, N. Wiik, G. Ambrosetti, A. Steinfeld, Spectral data of specular reflectance, narrow-angle transmittance and angle-resolved surface scattering of materials for solar concentrators, *Data in Brief*. 6 (2016) 184–188. <https://doi.org/10.1016/j.dib.2015.11.059>.
- [52] M. Cardona, P.Y. Yu, Optical Properties of Semiconductors, *Comprehensive Semiconductor Science and Technology*. (2011) 125–195. <https://doi.org/10.1016/B978-0-44-453153-7.00073-0>.
- [53] P. Zorabedian, Tunable External-Cavity Semiconductor Lasers, *Tunable Lasers Handbook*. (1995) 349–442. <https://doi.org/10.1016/B978-012222695-3/50009-X>.
- [54] C.J.R. Sheppard, Approximate calculation of the reflection coefficient from a stratified medium, *Pure Appl. Opt.* 4 (1995) 665–669. <https://doi.org/10.1088/0963-9659/4/5/018>.
- [55] L. Dumas, E. Quesnel, F. Pierre, F. Bertin, Optical properties of magnesium fluoride thin films produced by argon ion-beam assisted deposition, *Journal of Vacuum Science &*

- Technology A: Vacuum, Surfaces, and Films. 20 (2002) 102–106.  
<https://doi.org/10.1116/1.1424276>.
- [56] C. Xin, C. Peng, Y. Xu, J. Wu, A novel route to prepare weather resistant, durable antireflective films for solar glass, *Solar Energy*. 93 (2013) 121–126.  
<https://doi.org/10.1016/j.solener.2013.04.006>.
- [57] K. St Clair, *The Secret Lives of Colour*, John Murray, London, 2016.
- [58] W. Zhang, J. Tu, W. Long, W. Lai, Y. Sheng, T. Guo, Preparation of SiO<sub>2</sub> anti-reflection coatings by sol-gel method, *Energy Procedia*. 130 (2017) 72–76.  
<https://doi.org/10.1016/j.egypro.2017.09.398>.
- [59] K.H. Nielsen, D.K. Orzol, S. Koynov, S. Carney, E. Hultstein, L. Wondraczek, Large area, low cost anti-reflective coating for solar glasses, *Solar Energy Materials and Solar Cells*. 128 (2014) 283–288. <https://doi.org/10.1016/j.solmat.2014.05.034>.
- [60] F. Sutter, M. Montecchi, H. von Dahlen, A. Fernández-García, M. Röger, The effect of incidence angle on the reflectance of solar mirrors, *Solar Energy Materials and Solar Cells*. 176 (2018) 119–133. <https://doi.org/10.1016/j.solmat.2017.11.029>.